SYNTHESIS AND CHARACTERIZATION OF Fe_3O_4@SiO_2 SUB-NANO CORE/SHELL WITH SiO_2 DERIVED FROM RICE HUSK ASH

Luong Huynh Vu Thanh, Tran Nguyen Phuong Lan, Tran Thi Bich Quyen, Ha Quoc Nam, Le Phuoc Bao Tho

College of Engineering Technology, Can Tho University;
lhvthanh@ctu.edu.vn, tnplan@ctu.edu.vn, ttbquyen@ctu.edu.vn,
namb1506951@student.ctu.edu.vn, thob1506972@student.ctu.edu.vn

Abstract - This study aims to synthesize and characterize Fe_3O_4@SiO_2 sub-nanoparticles (SNPs) with high saturation magnetization (SM). The research process was conducted in simple and environmentally friendly conditions. The results of ultraviolet-visible (UV-Vis) spectroscopy and X-ray diffraction (XRD) analysis presented that the Fe_3O_4@SiO_2 SNPs were well formed and the phase change of Fe_3O_4 NPs did not happen in Fe_3O_4@SiO_2 SNPs. Transmission electron microscope (TEM) analysis showed that the Fe_3O_4@SiO_2 SNPs are in a fairly spherical shape with a core/shell structure and a diameter in a range of 100 nm to 500 nm. Fourier transform infrared spectrometry (FT-IR) spectra of Fe_3O_4@SiO_2 SNPs presented some absorption peaks indicating the existence of Si-O-Si, O-Si-O, Fe-O and Fe-O-Si. The SM of Fe_3O_4 particles and Fe_3O_4@SiO_2 SNPs determined via vibrating sample magnetometer (VSM) were 50.9 emu.g^{-1} and 19.5 emu.g^{-1}, respectively. All the above results provide clear evidence that the Fe_3O_4 particles were coated by SiO_2 to form sub-nano core/ shell with great SM.

Key words - Fe_3O_4@SiO_2; core-shell structure; saturation magnetization; rice husk ash

1. Introduction

Nowadays, Fe_3O_4 nano particles (NPs) have attracted much research interest for application in biomedical fields which consist of targeted drug delivery and immunoassays [1-3], carrier for enzyme immobilization for different uses [4-6]. Fe_3O_4 NPs with chemically stable, biocompatible and highly dispersible in various pH liquid media are mostly required for biomedical applications [7-9]. Methods for preparing magnetic nanoparticles including solid state reaction [10], sol–gel [11], co-precipitation [12], hydrothermal processes [13], and ultrasonic method [14] have been reported widely in literature. However, the bare Fe_3O_4 NPs are highly sensitive to acidic and oxidative conditions; thus, coating of Fe_3O_4 NPs with SiO_2 will also avoid the agglomeration and protect them from dissolution in acidic solution.

Polymer [15], noble metals [16] and silica [17, 18] have been discovered in recent years for use as the coating materials. Among those materials, silica is considered as one of the most promising candidates because it not only protects Fe_3O_4 NPs from oxidation and agglomeration, but also can be compatible with various chemicals and molecules for bio-conjugations due to its unique surface chemistry [19]. The silica shell in the Stöber method [20] is formed through the hydrolysis and condensation of silane precursor, namely tetraethyl orthosilicate (TEOs). The formation of large aggregates and polydispersed products is inevitable due to the high and uncontainable hydrolysis rate of TEOs and the quite low critical concentration for homogeneous nucleation of silica [21].

Although the above method is normally used for silica coating, it involves alcohol–water–ammonia as the media and TEOs as the silane monomers, resulting in a complex and expensive coating process. Silica that may be produced by treating rice husk ash (RHA) with sodium hydroxide and chloric acid has been repored for preparation of the shell coated Fe_3O_4 NPs. RHA is a solid waste of agricultural products and can be potentially used as row material for preparation of new silica-based materials due to high content of silica (80-90%) [22]. In this work, synthesis of Fe_3O_4@SiO_2 sub-nanoparticles (SNPs) with SiO_2 from RHA is reported in a non-alcohol solution and without any expensive precursors and organic solvents.

2. Experiment

2.1. Materials

Ferric chloride hexahydrate ($FeCl_3.6H_2O$), sodium hydroxide (NaOH), chloric acid (HCl), and ammonium hydroxide (NH_4OH) are reagent-grade and purchased from Xilong Chemicals. Sodium borohydride ($NaBH_4$) and poly vinyl pyrrolidone (PVP) were obtained from Sigma-Aldrich. All chemicals were used without further purification. For the coating experiment, SiO_2 extracted from RHA purchased at Can Tho city, Vietnam was used.

2.2. Synthesis

2.2.1. SiO_2 particles preparation

The SiO_2 particles were synthesized by chemical reduction technique [23]. The initial step is extraction of SiO_2 from RHA as Na_2SiO_3 using aqueous NaOH. Ten gram of RHA was first stirred with 100 mL of NaOH 3 M at 200^{o}C for 2 h. A yellow viscous solution was obtained after filtration of the reacted slurry. The second step of the process is SiO_2 precipitation. The SiO_2 particles were precipitated from Na_2SiO_3 solution by acidification using HCl 2.5 M. The addition of the acid was done very slowly till pH of solution reached 6.0. The white SiO_2 precipitates were obtained. This SiO_2 was subjected to a successive washing with distilled water. Finally, the wet precipitates were dried at 60^{o}C in an oven for 24 h.

2.2.2. Fe_3O_4@SiO_2 SNPs synthesis

Firstly, 0.054 g $FeCl_3.6H_2O$ was dissolved in 50 mL of PVP 1% with stirring, and then 50 mL of $NaBH_4$ 0.5 M was added to the obtained solution. In the meantime, temperature was increased to 80^{o}C for 15 min. The color of solution changed from bright to dark bright after that. In sequence, 0.02 g of SiO_2 was added to the obtained solution and pH was maintained during the synthesis, around 12.0 by adding NH_4OH 25%.

The Fe_3O_4@SiO_2 NPs were synthesized for 2h at the above temperature, sequently cooled down to room temperature and then given multiple washing with distilled water and absolute ethanol. The product was dried in vacuum condition of 50°C and 0.5 atm for 6h.

2.2.3. Synthesized material characterization

The as-synthesized materials were subsequently characterized by UV-Vis spectroscopy measured by UV-1800 Shimadzu. The size and morphologic analyses of Fe_3O_4 NPs and Fe_3O_4@SiO_2 NPs were obtained using an Instrument Jem 1400 transmission electron microscope (TEM). The crystalline structures of Fe_3O_4 NPs and Fe_3O_4@SiO_2 NPs were investigated by XRD measured by a D8-Advance using Cu-Kα radiation (λ=0.15405 nm).The Nicolet 6700 Fourier transform infrared (FT-IR) spectroscopy were employed to analyze the functional groups, as well as the interaction between SiO_2 and Fe_3O_4 NPs. Magnetic properties of the Fe_3O_4 NPs and Fe_3O_4@SiO_2 NPs were studied by using the vibrating sample magnetometer (VSM), quantum design 14 T PPMS.

3. Results and discussion

3.1. Prepareation of Fe_3O_4@SiO_2 SNPs

The process for synthesizing Fe_3O_4@SiO_2 SNPs with SiO_2 dirived from RHA is shown in Figure 1. The PVP-grafted Fe_3O_4 NPs were synthesized by web chemical reduction of $FeCl_3$ and reducting agent $NaBH_4$. Poly vinyl pyrrolidone molecules attached to the surface of Fe_3O_4 NPs prevented random agglomeration of particles andfacilitated the cluster formation. The PVP-grafted Fe_3O_4 NPs prepared via this method has a number of hydroxyl groups on the surface. The silica shell coated Fe_3O_4 NPs was achieved by the reaction between silicon element and the hydroxyl groups on the surface of magnetite.

3.2. Ultra Violet – Visible

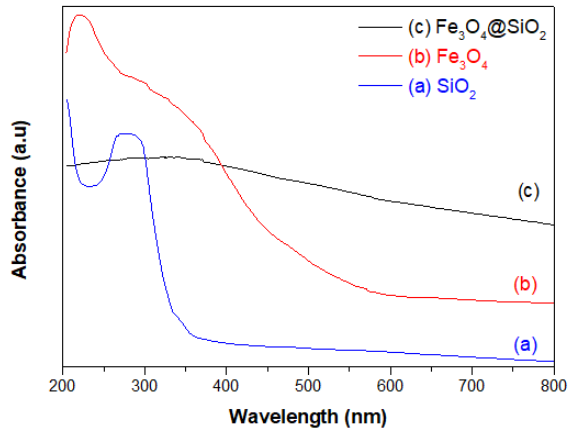

Figure 1. *UV-Vis adsorption spectra of different of (a) SiO_2, (b) Fe_3O_4 NPs and (c) Fe_3O_4@SiO_2 SNPs*

The UV-Vis absorption spectra of different samples in water are illustrated in Figure 2. The absorption spectra of SiO_2 showed no significant peaks. No obvious peaks appeared in the spectra of Fe_3O_4 NPs and SiO_2. However, a board featureless peak can be observed at 380 nm in the spectrum of Fe_3O_4@SiO_2 SNPs. The broad peak indicated the core-shell structure of Fe_3O_4@SiO_2 SNPs [24, 25], and this peak may come from the changes of band gap caused by the quantum size effect and surface effect of macrostructure, indicating that SiO_2-coated Fe_3O_4 NPs were successfully synthesized.

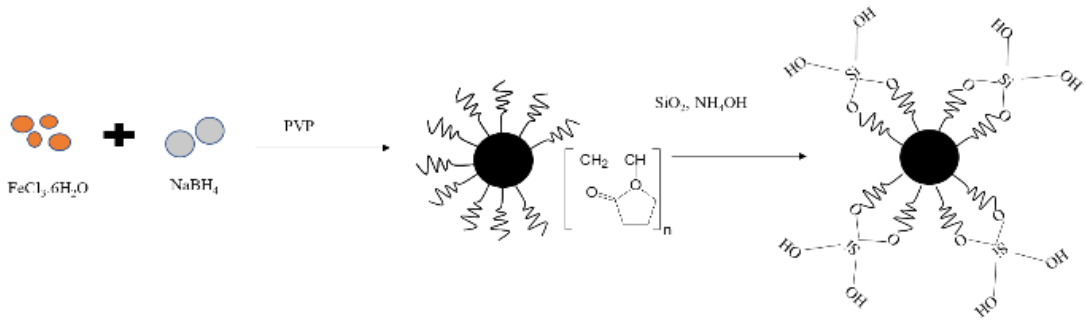

Figure 2. *Preparation of silica coated magnetic nanoparticles*

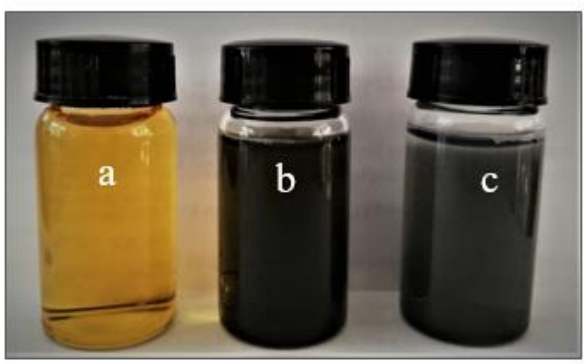

Figure 3. *The color change of solution $FeCl_3.6H_2O$ (a), Fe_3O_4 NPs (b) and sub-nano Fe_3O_4@SiO_2 (c)*

Figure 3a presented a typical yellow solution of Fe(III). As soon as the reducing agent ($NaBH_4$) was added to the solution, a black precipitate was formed (Figure 3b). A similar phenomenon was also observed in the study of Basavegowda, N. et al. [26]. However, the color of the solution was slightly changed from a dark black to a light black (Figure 3c) when SiO_2 coated on the surface of the Fe_3O_4 core. This color change is caused by an increase in the particle size due to coating SiO_2 around the Fe_3O_4 NPs.

3.3. X-ray powder diffraction

In terms of nano-material synthesis, phase identification and crystalline structures of NPs is one of key uses of XRD. The XRD patterns of SiO_2, Fe_3O_4 and

Fe_3O_4@SiO_2 are shown in Figure 4. As shown in Figure 4a, an amorphous peak of precipitated SiO_2 with the equivalent Bragg angle at 2θ = 22° – 23° was recorded [27, 28]. In the meantime, the crystallinity and structures of Fe_3O_4 NPs and Fe_3O_4@SiO_2 SNPs were determined via their XRD patterns in Figure 4b. The main peaks at 2θ = 30.3°; 35.7°; 43.4°; 53.8°; 57.3°; 62.9° refer to (200); (311); (400); (422); (511); (440) plane of cubic inverse spinel Fe_3O_4 NPs [19, 29], respectively. The lattice parameter is in good agreement to the standard data (JCPDS No. 00-001-1111). No other significant peaks of FeOOH, Fe_2O_3 can be observed in the XRD pattern of Fe_3O_4@SiO_2 SNPs.

Additionally, the XRD results of the coated magnetite material reveal comparatively broad diffraction peak at 2θ = 22° – 23° and lower peak intensity in comparison to peak intensity of non-coating one, which proves SiO_2 coating on surface of the magnetite material. Similar result was found in the study of Nuryono et al. (2014) when the crystallite was coated by silica from RHA [30]. Thus, XRD further confirmed the formation of Fe_3O_4@SiO_2 SNPs. This also revealed that the phase change of Fe_3O_4 NPs did not take place in Fe_3O_4@SiO_2 SNPs.

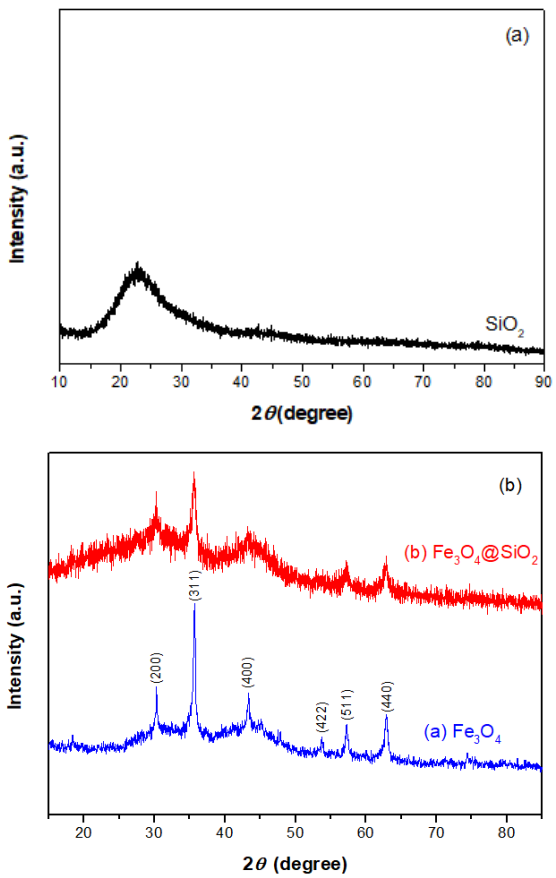

Figure 4. *XRD patterns of (a) SiO_2 and (b) Fe_3O_4 NPs and Fe_3O_4@SiO_2 NPs*

The particles' size was calculated from the XRD data using Scherrer's equation:

$$D = \frac{k.\lambda}{\beta.\cos(\theta)} \text{ (Å)} \quad (1)$$

where D is particles'size, k is the grain shape factor taken as unity contemplating that the particles are spherical in shape, λ is the incident X-ray wavelength of Cu-Ka radiation and θ is the Bragg's angle, β is the broadening of diffraction line measured at half maximum intensity (radians).

Different Bragg's angles of Fe_3O_4@SiO_2 SNPs had been employed to calculate crystallite size, and the result is presented in Table 1. With six Bragg's angle used to calculate crystallite size, the obtained crystallite size varied from 16.4 nm to 38.3 nm, and the average crystallite size was determined at 26.04 nm.

Table 1. *X-ray diffraction measurements of Fe_3O_4@SiO_2 NPs for evaluating average crystallite size*

Peak	2θ (deg)	hkl	FWHM (radians)	D (nm)
1	30.3	(200)	0.00462	31.1
2	35.7	(311)	0.00614	23.7
3	43.4	(400)	0.00567	26.3
4	53.8	(422)	0.00406	38.3
5	57.3	(511)	0.00770	20.5
6	62.9	(440)	0.00993	16.4

3.4. Fourier transform infrared

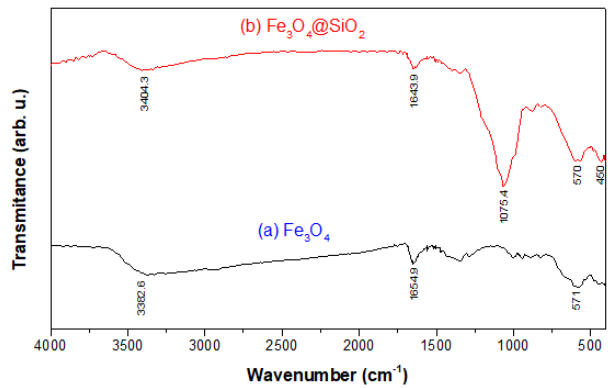

Figure 5. *FT-IR spectra of (a) Fe_3O_4 NPs and (b) Fe_3O_4@SiO_2 NPs*

Fourier transform infrared analysis was proved to be useful to characteristic of Fe_3O_4@SiO_2 NPs. Pure Fe_3O_4 NPs and Fe_3O_4@SiO_2 SNPs were analyzed by FT-IR and their IR spectra were compared and presented in Figure 5. Typical bondings of these two materials were also summarized and shown in Table 2. The characteristic vibration of Fe-O at 570cm^{-1} and 571cm^{-1} were respectively observed at IR spectrum of Fe_3O_4 NPs and Fe_3O_4@SiO_2 SNPs. It proves that the Fe_3O_4@SiO_2 SNPs contained Fe_3O_4 NPs [29]. However, the vibration of Si-O-Si or O-Si-O can be only observed in IR spectrum of Fe_3O_4@SiO_2 NPs. In fact, the absorption band with high-intensity at 1075.4 cm^{-1} is due to the asymmetric stretching bonds of Si-O-Si. The band at 450 cm^{-1} is consistent with Si-O-Si or O-Si-O [31]. These above results confirm that Fe_3O_4 NPs were coated by SiO_2 to form Fe_3O_4@SiO_2 SNPs. Besides those characteristic vibration, some other vibrations such as O-H bending vibration, O-H stretching vibration appeared at at 1654.9 cm^{-1}, 3382.6 cm^{-1} and 1643.9 cm^{-1}, 3404.3 cm^{-1} in both IR spectra of Fe_3O_4 NPs and Fe_3O_4@SiO_2 SNPs respectively [31, 32].

Table 2. *Data analysis results of FT-IR spectra of (a) Fe_3O_4 NPs and (b) Fe_3O_4@SiO_2 NPs*

No	Functional group	Wavenumber (cm^{-1})	Wavenumber of Fe_3O_4 (cm^{-1})	Wavenumber of Fe_3O_4@SiO_2 (cm^{-1})	References
1	O-H stretching	3650-3200	3382.6	3404.3	[1]
2	O-H	1640-3483	1654.9	1643.9	[2]
3	Si-O-Si stretching vibration Fe-O-Si stretching	1370-1380	-	1075.4	[1]
4	Fe-O Si-O-Fe	570	571	570	[3, 4]
5	O-Si-O or Si-O-Si	461	-	450	[3, 4]

3.5. Transmission electron microscope

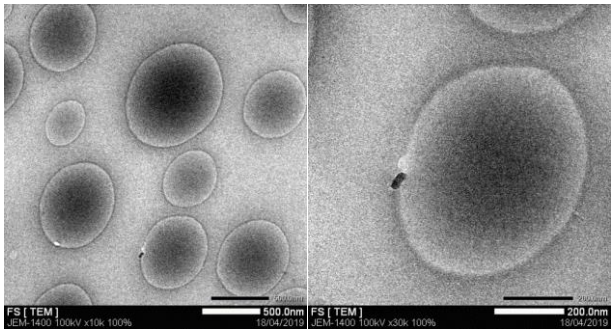

Figure 6. *TEM images of Fe_3O_4@SiO_2 NPs at different resolutions*

TEM analysis was employed to determine surface morphology, size and dispersion of the as-prepared Fe_3O_4@SiO_2 SNPs. It also helps to illustrate the core-shell structure of a material. Figure 6 shows the TEM images of the as-synthesized Fe_3O_4@SiO_2 SNPs at various resolutions. The result indicates that the as-prepared Fe_3O_4@SiO_2 SNPs are almost spherical in shape. The diameter of the particles mainly ranged from 100 nm to 500 nm, which is similar to the studies of Subhan et al. (2019) and Rahman et al. (2015), although the synthesis of core-shell Fe_3O_4@SiO_2 SNPs was not performed by the Stober method [33, 34]. The Fe_3O_4@SiO_2 SNPs in this investigation formed a well-defined core-shell structure with dark contrast of the crystalline nature of Fe_3O_4 and light contrast of SiO_2. This well-defined core-shell structure was proved to be highly defensive for avoiding the corrosion, keeping a stable dispersion and making the magnetic core stable.

3.6. Vibrating sample magnetometer

The investigation of the magnetic property was conducted through the analysis of VSM. Figure 7 revealed that no hysteresis in the magnetization curves can be observed. The remnant magnetization and coercivity field cannot be found from these curves as well. It confirms that Fe_3O_4@SiO_2 core/shell SNPs are super-paramagnetic. Both curves demonstrated super-paramagnetic property with a saturation magnetization (Ms) of 50.9 $emu.g^{-1}$ for Fe_3O_4 and 19.5 $emu.g^{-1}$ for Fe_3O_4@SiO_2 NPs. As Fe_3O_4@SiO_2 SNPs were synthesized, SiO_2 shells would shield the magnetism of Fe_3O_4 NPs that led to a decrease in Ms of Fe_3O_4@SiO_2 SNPs [35, 36]. In the study of Gao et al. (2011), the Ms of Fe_3O_4@SiO_2 SNPs changed from 12.7 to 6.3, 4.3, 3.1 and 2.4 $emu.g^{-1}$ with variation of TEOs adding from 1 to 2, 3, 5 and 8 mL [37]. Similarly, the study of Shengxiao et al. (2013) showed that the Ms of Fe_3O_4 and Fe_3O_4@SiO_2 SNPs changed from 55.05 $emu.g^{-1}$ to 25.45 when SiO_2 was coated on Fe_3O_4 nanoparticles through sodium silicate hydrolyzing under acid condition [38]. This again confirms that the outer part of the core-shell structure decreases the Ms. In other words, the thinner the outer part thickness is, the higher the Ms is. In terms of green chemistry, the Fe_3O_4@SiO_2 SNPs with well-defined core-shell structure and high Ms in this study were obtained without adding any TEOs.

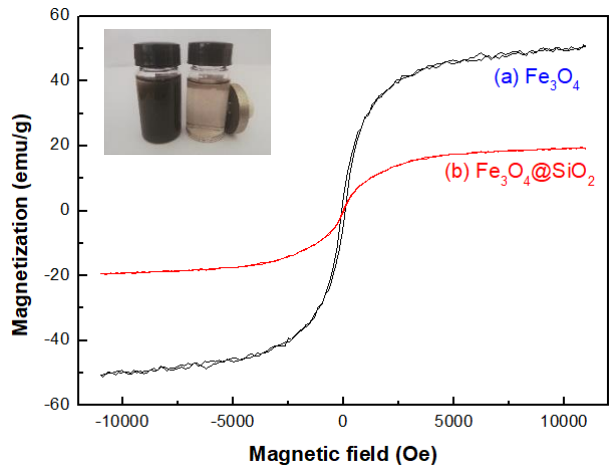

Figure 7. *Vibrating sample magnetometer magnetization curves of Fe_3O_4 NPs and Fe_3O_4@SiO_2 NPs*

4. Conclusions

The Fe_3O_4@SiO_2 SNPs with a core-shell structure in this study were well prepared via a simple, efficient and inexpensive process. The supporting agent – SiO_2 extracted from RHA was to work in forming the shell of Fe_3O_4@SiO_2 SNPs. The analyses of TEM, FTIR and XRD showed that the obtained NPs are in a fairly spherical shape and its size is about 100-500 nm. The well-defined core-shell structure of Fe_3O_4@SiO_2 SNPs was successfully synthesized without any phase change of Fe_3O_4 NPs. The Fe_3O_4@SiO_2 SNPs presented super-paramagnetic property with high saturation magnetization of 19.5 $emu.g^{-1}$. These core-shell Fe_3O_4@SiO_2 SNPs are highly promising for much needed bio-conjugation applications.

REFERENCES

[1] J.H. Lee, Y.w. Jun, S.I. Yeon, J.S. Shin, J. Cheon, "Dual-mode nanoparticle probes for high-performance magnetic resonance and fluorescence imaging of neuroblastoma", *Angewandte Chemie*, 118(48), 2006, 8340-8342.

[2] F. Hu, L. Wei, Z. Zhou, Y. Ran, Z. Li, M. Gao, "Preparation of biocompatible magnetite nanocrystals for in vivo magnetic resonance detection of cancer", *Advanced Materials*, 18(19), 2006, 2553-2556.

[3] N. Nasongkla, E. Bey, J. Ren, H. Ai, C. Khemtong, J.S. Guthi, S.-F. Chin, A.D. Sherry, D.A. Boothman, J. Gao, "Multifunctional polymeric micelles as cancer-targeted, MRI-ultrasensitive drug delivery systems", *Nano letters*, 6(11), 2006, 2427-2430.

[4] S. Kumar, A.K. Jana, I. Dhamija, Y. Singla, M. Maiti, "Preparation, characterization and targeted delivery of serratiopeptidase immobilized on amino-functionalized magnetic nanoparticles", *European Journal of Pharmaceutics and Biopharmaceutics*, 85(3), 2013, 413-426.

[5] J. Jordan, C.S. Kumar, C. Theegala, "Preparation and characterization of cellulase-bound magnetite nanoparticles", *Journal of Molecular Catalysis B: Enzymatic*, 68(2), 2011, 139-146.

[6] Y.-T. Zhu, X.-Y. Ren, Y.-M. Liu, Y. Wei, L.-S. Qing, X. Liao, "Covalent immobilization of porcine pancreatic lipase on carboxyl-activated magnetic nanoparticles: characterization and application for enzymatic inhibition assays", *Materials Science and Engineering: C*, 38, 2014, 278-285.

[7] A.H. Lu, E.e.L. Salabas, F. Schüth, "Magnetic nanoparticles: synthesis, protection, functionalization, and application", *Angewandte Chemie International Edition*, 46(8), 2007, 1222-1244.

[8] C. Hui, C. Shen, J. Tian, L. Bao, H. Ding, C. Li, Y. Tian, X. Shi, H.-J. Gao, "Core-shell Fe_3O_4@SiO_2 nanoparticles synthesized with well-dispersed hydrophilic Fe_3O_4 seeds", *Nanoscale*, 3(2), 2011, 701-705.

[9] Y. Lu, Y. Yin, B.T. Mayers, Y. Xia, "Modifying the surface properties of superparamagnetic iron oxide nanoparticles through a sol−gel approach", *Nano letters*, 2(3), 2002, 183-186.

[10] G. Chandrasekaran, P.N. Sebastian, "Magnetic study of $Zn_xMg_{1-x}Fe_2O_4$ mixed ferrites", *Materials Letters*, 37(1-2), 1998, 17-20.

[11] W.C. Kim, S.J. Kim, S.W. Lee, C.S. Kim, "Growth of ultrafine NiZnCu ferrite and magnetic properties by a sol–gel method", *Journal of magnetism and magnetic materials*, 226, 2001, 1418-1420.

[12] A. Ataie, S. Heshmati-Manesh, "Synthesis of ultra-fine particles of strontium hexaferrite by a modified co-precipitation method", *Journal of the European Ceramic Society*, 21(10-11), 2001, 1951-1955.

[13] S.-H. Yu, T. Fujino, M. Yoshimura, "Hydrothermal synthesis of $ZnFe_2O_4$ ultrafine particles with high magnetization", *Journal of Magnetism and Magnetic Materials*, 256(1-3), 2003, 420-424.

[14] X. Lu, H. Mao, D. Chao, W. Zhang, Y. Wei, "Ultrasonic synthesis of polyaniline nanotubes containing Fe_3O_4 nanoparticles", *Journal of Solid State Chemistry*, 179(8), 2006, 2609-2615.

[15] R. Qiao, C. Yang, M. Gao, "Superparamagnetic iron oxide nanoparticles: from preparations to in vivo MRI applications", *Journal of Materials Chemistry*, 19(35), 2009, 6274-6293.

[16] Z. Xu, Y. Hou, S. Sun, "Magnetic core/shell Fe_3O_4/Au and Fe_3O_4/Au/Ag nanoparticles with tunable plasmonic properties", *Journal of the American Chemical Society*, 129(28), 2007, 8698-8699.

[17] J. Ge, Q. Zhang, T. Zhang, Y. Yin, "Core–satellite nanocomposite catalysts protected by a porous silica shell: controllable reactivity, high stability, and magnetic recyclability", *Angewandte Chemie International Edition*, 47(46), 2008, 8924-8928.

[18] Y. Deng, C. Deng, D. Qi, C. Liu, J. Liu, X. Zhang, D. Zhao, "Synthesis of core/shell colloidal magnetic zeolite microspheres for the immobilization of trypsin", *Advanced Materials*, 21(13), 2009, 1377-1382.

[19] A.-L. Morel, S.I. Nikitenko, K. Gionnet, A. Wattiaux, J. Lai-Kee-Him, C. Labrugere, B. Chevalier, G. Deleris, C. Petibois, A. Brisson, "Sonochemical approach to the synthesis of Fe_3O_4@SiO_2 core−shell nanoparticles with tunable properties", *ACS nano*, 2(5), 2008, 847-856.

[20] W. Stöber, A. Fink, E. Bohn, "Controlled growth of monodisperse silica spheres in the micron size range", *Journal of colloid and interface science*, 26(1), 1968, 62-69.

[21] X. Jiang, T. Herricks, Y. Xia, "Monodispersed spherical colloids of titania: synthesis, characterization, and crystallization", *Advanced Materials*, 15(14), 2003, 1205-1209.

[22] S.C.W. Sakti, D. Siswanta, Adsorption of gold (III) on ionic imprinted amino-silica hybrid prepared from rice hull ash, *Pure and Applied Chemistry* 85(1) (2012) 211-223.

[23] N.T. Tuấn, N.H.M. Phú, H.N.T. Tân, P.T.B. Thảo, N.T.K. Chi, L.V. Nhạn, N.T. Tuân, T.X. Anh, Tổng hợp hạt nano SiO2 từ tro vỏ trấu bằng phương pháp kết tủa, *Tạp chí Khoa học Trường Đại học Cần Thơ* (2014) 120-124.

[24] N. Gan, P. Xiong, J. Wang, T. Li, F. Hu, Y. Cao, L. Zheng, "A novel signal-amplified immunoassay for the detection of C-reactive protein using HRP-doped magnetic nanoparticles as labels with the electrochemical quartz crystal microbalance as a detector", *Journal of analytical methods in chemistry*, 2013.

[25] Y. Wang, X. Peng, J. Shi, X. Tang, J. Jiang, W. Liu, "Highly selective fluorescent chemosensor for Zn^{2+} derived from inorganic-organic hybrid magnetic core/shell Fe_3O_4@SiO_2 nanoparticles", *Nanoscale research letters*, 7(1), 2012, 86.

[26] N. Basavegowda, K.B.S. Magar, K. Mishra, Y.R. Lee, "Green fabrication of ferromagnetic Fe_3O_4 nanoparticles and their novel catalytic applications for the synthesis of biologically interesting benzoxazinone and benzthioxazinone derivatives", *New Journal of Chemistry*, 38(11), 2014, 5415-5420.

[27] S. Venkateswaran, R. Yuvakkumar, V. Rajendran, "Nano silicon from nano silica using natural resource (RHA) for solar cell fabrication", *Phosphorus, Sulfur, and Silicon and the Related Elements*, 188(9), 2013, 1178-1193.

[28] M. Choolaei, A.M. Rashidi, M. Ardjmand, A. Yadegari, H. Soltanian, "The effect of nanosilica on the physical properties of oil well cement", *Materials Science and Engineering: A*, 538, 2012, 288-294.

[29] S. Wang, J. Tang, H. Zhao, J. Wan, K. Chen, "Synthesis of magnetite–silica core–shell nanoparticles via direct silicon oxidation", *Journal of colloid and interface science*, 432, 2014, 43-46.

[30] N. Nuryono, N.M. Rosiati, B. Rusdiarso, S.C.W. Sakti, S. Tanaka, Coating of magnetite with mercapto modified rice hull ash silica in a one-pot process, SpringerPlus 3(1) (2014) 515.

[31] Y. Chen, Z. Peng, L.X. Kong, M.F. Huang, P.W. Li, "Natural rubber nanocomposite reinforced with nano silica", *Polymer Engineering & Science*, 48(9), 2008, 1674-1677.

[32] A.M. Said, M.S. Zeidan, M. Bassuoni, Y. Tian, "Properties of concrete incorporating nano-silica", *Construction and Building Materials*, 36, 2012, 838-844.

[33] F. Subhan, S. Aslam, Z. Yan, M. Khan, U. Etim, M. Naeem, "Effective adsorptive performance of Fe_3O_4@SiO_2 core-shell spheres for methylene blue: kinetics, isotherm and mechanism", *Journal of Porous Materials*, 2019, 1-10.

[34] Z.U. Rahman, T. Zhang, S. Cui, D. Wang, "Preparation and characterization of magnetic nanocomposite catalysts with double Au nanoparticle layers", *RSC Advances*, 5(121), 2015, 99697-99705.

[35] L. Wang, C. Shen, Y. Cao, "PVP modified Fe_3O_4@SiO_2 nanoparticles as a new adsorbent for hydrophobic substances", *Journal of Physics and Chemistry of Solids*, 133, 2019, 28-34.

[36] M. Mostafaei, S.N. Hosseini, M. Khatami, A. Javidanbardan, A.A. Sepahy, E. Asadi, "Isolation of recombinant Hepatitis B surface antigen with antibody-conjugated superparamagnetic Fe_3O_4/SiO_2 core-shell nanoparticles", *Protein expression and purification*, 145, 2018, 1-6.

[37] M. Gao, W. Li, J. Dong, Z. Zhang, B. Yang, Synthesis and characterization of superparamagnetic Fe_3O_4@SiO_2 core-shell composite nanoparticles, *World Journal of Condensed Matter Physics* 1(02) (2011) 49.

[38] Y. Zhang, Q. Xu, S. Zhang, J. Liu, J. Zhou, H. Xu, H. Xiao, J. Li, Preparation of thiol-modified Fe_3O_4@SiO_2 nanoparticles and their application for gold recovery from dilute solution, *Separation and Purification Technology* 116 (2013) 391-397.

(The Board of Editors received the paper on 18/9/2019, its review was completed on 20/12/2019)